Check for updates

View Article Online
View Journal

Analyst

Accepted Manuscript

This article can be cited before page numbers have been issued, to do this please use: S. Ding, Y. Xu, Q. Liu, H. Gu, A. Zhu and G. Shi, *Analyst*, 2020, DOI: 10.1039/C9AN02285F.

This is an Accepted Manuscript, which has been through the Royal Society of Chemistry peer review process and has been accepted for publication.

Accepted Manuscripts are published online shortly after acceptance, before technical editing, formatting and proof reading. Using this free service, authors can make their results available to the community, in citable form, before we publish the edited article. We will replace this Accepted Manuscript with the edited and formatted Advance Article as soon as it is available.

You can find more information about Accepted Manuscripts in the Information for Authors.

Please note that technical editing may introduce minor changes to the text and/or graphics, which may alter content. The journal's standard Terms & Conditions and the Ethical guidelines still apply. In no event shall the Royal Society of Chemistry be held responsible for any errors or omissions in this Accepted Manuscript or any consequences arising from the use of any information it contains.

Please do not adjust margins

View Article Online
DOI: 10.1039/C9AN02285F

ARTICLE

Interface engineering of microelectrodes toward ultrasensitive monitoring of β-amyloid peptides in cerebrospinal fluid in Alzheimer's disease

Received 00th January 20xx,
Accepted 00th January 20xx

DOI: 10.1039/x0xx00000x

Shushu Ding,[†a] Yunxia Xu,[†a] Qi Liu,[a] Hui Gu,[b] Anwei Zhu*[a] and Guoyue Shi*[a]

Ultrasensitive detection of monomeric β-amyloid peptides (Aβ) is of fundamental significance for studying the pathological progression of Alzheimer's disease (AD). In this article, by facilely engineering gold microelectrode interface, we developed a novel electrochemical biosensor for sensitive and selective monitoring of Aβ monomers in cerebrospinal fluid (CSF). Through the specific Cu^{2+}-Aβ-hemin coordination, Aβ directed the assembly of Cu^{2+}-PEI/AuNPs-hemin nanoprobes into network aggregates on microelectrode interface, which promoted the enrichment of Aβ monomers on microelectrode. Furthermore, the AuNP aggregate promote the deposition of silver nanoparticles, which were utilized for electrochemical stripping analysis of Aβ monomer. The proposed method displayed ultra-sensitivity for Aβ monomers with the detection limit down to 0.2 pM. Besides, high selectivity toward Aβ monomers was observed. Theses remarkable analytical performance made the electrochemical biosensor available for evaluating the dynamic change of Aβ monomers level in CSF of live mice with AD, promoting the investigation of the role that Aβ monomers play in brain events.

Introduction

Alzheimer's disease (AD) is a neurodegenerative disorder that is the most common cause of dementia. Aggregation of β-amyloid peptide (Aβ) is considered to be the critical event in the pathogenesis of AD.[1-3] Aβ monomers in their native forms are continuously produced by sequential cleavage of amyloid precursor protein and secreted into the cerebrospinal fluid (CSF) of the central nervous system (CNS). However, they trended to aggregate into oligomers or fibrils under various conditions, promoting the progression of AD.[4,5] Thus, the level of Aβ monomers in CSF was suggested to correlate with the cognitive impairment of AD and quantitatively measuring Aβ monomers in CSF is crucial for AD clinical studies. However, several challenges still existed: (1) to avoid risks of infection at the puncture site and damage to the brain and spinal cord, extremely small volume of CSF was taking out from CNS immediately, (2) the CSF samples possess low-abundance Aβ monomers, (3) miscellaneous interferences are present in CSF. Therefore, it is urgent to develop an effective method for sensitive and selective detection of Aβ monomers in CSF.

The current methods for detecting Aβ monomers mostly rely on biochemical assays such as polyacrylamide gel electrophoresis, immunoprecipitation, enzyme-linked immunosorbent assay. However, the limitations of these techniques were time-consuming, the requirement of relatively expensive enzyme-linked antibody and toxic reagents for detection.[6-8] Although non-biochemical techniques including surface plasmon resonance, mass spectrometry and capillary electrophoresis have been employed, they are labor intensive and require complicated instruments.[9-12] In this regard, colorimetric assays with simple manipulation have been developed.[13,14] However, the majority of colorimetry exhibited poor sensitivity for Aβ monomers in CSF.

Recently, electrochemical biosensors have been widely used in clinical diagnosis because of their low cost, simplicity and potential ability for on-site analysis.[15-17] Especially, the recent development of microelectrodes with small size have emerged as ideal analytical tools for the detection of clinical samples with small volume.[18,19] However, the slow diffusion rate of Aβ monomers limited their enrichment at the electrode surface, which necessitates the fabrication of microelectrodes with high sensitivity. Currently, metal nanoparticles have been widely employed as signal amplification strategy for the development of ultrasensitive electrochemical methods.[20] Firstly, metal nanoparticles can be used as electrochemical probes due to good electrical conductivity and can provide well-defined electrochemical signal. Secondly, these metal nanoparticles exhibited a superficial property similar to metal electrodes, which can be easily functionalized and engineered to improve the performance of the electrochemical sensors.[21,22] As far as we know, the exploration of metal nanoparticles on

[a] School of Chemistry and Molecular Engineering, Shanghai Key Laboratory for Urban Ecological Processes and Eco-Restoration, East China Normal University, 500 Dongchuan Road, Shanghai 200241, People's Republic of China.
[b] School of Chemistry and Chemical Engineering, Key Laboratory of Theoretical Organic Chemistry and Functional Molecule of Ministry of Education, Hunan University of Science and Technology, Xiangtan, Hunan, 411201, People's Republic of China.
† These authors contributed equally to this work.
Electronic Supplementary Information (ESI) available: [details of any supplementary information available should be included here]. See DOI: 10.1039/x0xx00000x

Published on 13 January 2020. Downloaded by Queen Mary, University of London on 1/13/2020 1:30:57 PM.

Analyst Accepted Manuscript

View Article Online DOI: 10.1039/C9AN02285E

Published on 13 January 2020. Downloaded by Queen Mary, University of London on 1/13/2020 1:30:57 PM.

microelectrode for monitoring Aβ monomers in CSF has never been reported.

Herein, we reported a new electrochemical biosensor for ultrasensitive monitoring of Aβ monomers (Figure 1) based on target-directed assembly of gold nanoparticles (AuNPs) on Au microelectrode interface. First, inspired by the important roles of heme and transition metal ions (i.e., Cu^{2+}) in Aβ metabolism,[23] dual-functionalized nanoprobes (Cu^{2+}-PEI/AuNPs-hemin nanoprobes) were prepared through attaching both Cu^{2+} and hemin onto the AuNPs surface. In the presence of Aβ monomers, double molecular recognitions between the nanoprobes and Aβ monomers occurred, forming Cu^{2+}-Aβ-hemin complex and resulting in AuNPs aggregation in solution. Then, the gold microelectrode was functionalized with hemin. Through Cu^{2+}-Aβ-hemin coordination, Aβ-mediated aggregation of Cu^{2+}-PEI/AuNPs-hemin nanoprobes in solution can be facilely initiated on the solid (microelectrode) - liquid (electrolyte) interface, resulting in the assembly of nanoprobes into network aggregates on the microelectrode surface.[24,25] Such architectures promoted the accumulation of Aβ monomers on microelectrodes. Besides, the assembly of AuNPs with large surface area provided abundant active sites for the in situ deposition of silver nanoparticles.[26-28] Through linear-sweep voltammetry (LSV), the amplified stripping signal of silver nanoparticles was employed for the electrochemical analysis of Aβ monomers.[29-31] Accordingly, this analytical method established a sensitive and selective method for monitoring dynamic changes of Aβ monomer in CSF of live mice. To the best of our knowledge, this is the first report of a gold microelectrode-based electrochemical biosensor for ultrasensitive monitoring of Aβ monomers associated with AD.

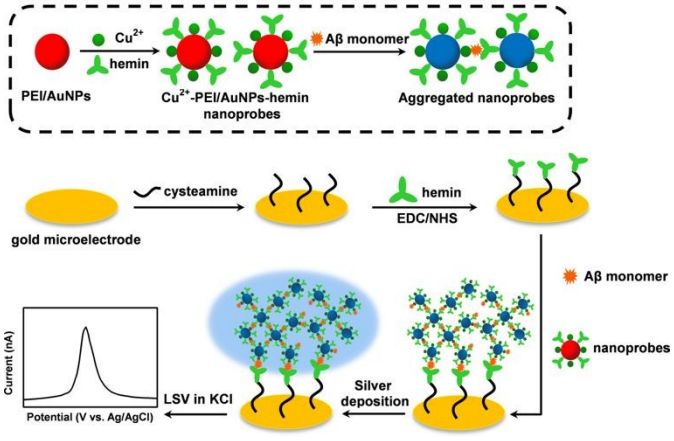

Figure 1. Schematic illustration of the electrochemical biosensor for measurement of Aβ monomers. The process of Aβ-directed aggregation of Cu^{2+}-PEI/AuNPs-hemin nanoprobes was transferred to the gold electrode surface and converted colorimetric assay into enhanced electrochemical analysis.

Experimental

Reagents and Materials

The β-amyloid peptides were obtained from ChinaPeptides Co., Ltd. (Shanghai, China). Cysteamine, 1-ethyl-3-(3-dimethylaminopropyl)carbodiimide hydrochloride (EDC) and metallic salts were bought from Aladdin. Chloroauric acid ($HAuCl_4 \cdot 4H_2O$) and copper (II) chloride were supplied by Sinopharm Chemical Reagent Co., Ltd. Branched polyethyleneimine (PEI, Mw=25 kDa), hemin, 1,1,1,3,3,3-hexafluoroisopropanol (HFIP), dimethyl sulfoxide (DMSO), silver enhancer solutions, N-hydroxysulfosuccinimide (NHS), glucose, ascorbate acid (AA), dopamine (DA), 5-hydroxytryptamine (5-HT), 3,4-dihydroxyphenylacetic acid (DOPAC), lactate, proteins and amino acids were purchased from Sigma-Aldrich. All aqueous solutions were prepared with Milli-Q water (18 $M\Omega \cdot cm^{-1}$).

Instrumentation and Apparatus

The UV-vis absorption spectra were acquired on a Shimadzu UV-1800 spectrometer. Transmission electron microscope (TEM) images were obtained with a JEOL JEM-2100 microscope. Scanning electron microscopy (SEM) images were taken by a HITACHI S-4800 scanning electron microscope. Zeta-potentials and dynamic light scattering (DLS) experiments were performed on a Malvern Zetasizer Nano ZS90. X-ray photoelectric spectroscopy (XPS) was carried on a Kratos Axis Ultra DLD spectrometer with Al Kα source (1486.6 eV). Electrochemical impedance spectroscopy (EIS) measurements were recorded on a Metrohm Autolab PGSTAT302N potentiostat-galvanostat. Linear sweep voltammetry (LSV) were collected by a CHI 660C electrochemical workstation (Shanghai, China). All electrochemical experiments were performed with a gold microelectrode as working electrode, Ag/AgCl electrode as reference electrode and a platinum wire as counter electrode.

Synthesis of the Cu^{2+}-PEI/AuNPs-hemin nanoprobes

Firstly, polyethylenimine (PEI) functionalized gold nanoparticles (PEI/AuNPs) were prepared as follows: 25 mL of deionized water and 1 mL of PEI (1%) were added to $HAuCl_4$ solution (1 g/10 mL, 100 μL) under vigorous stir. After stirring at ambient temperature for 6 h, the color of the solution changed to wine red.[32] The resulting PEI/AuNPs solution was stored at 4 ℃ overnight. For further functionalization, the PEI/AuNPs solution was centrifuged at 4 ℃, 12000 r/min for 10 min, followed by redispersing in 26 mL of deionized water. Then, EDC/NHS activated hemin (0.25 mM, 3 μL) and $CuCl_2$ (40 mM, 3 μL) were added to 200 μL of PEI/AuNPs solution in succession. After incubation for 1 h, the mixture was centrifuged and resuspended with 200 μL water to obtain the Cu^{2+}-PEI/AuNPs-hemin nanoprobes. The resulting nanoprobes solution was stored at 4 °C before use.

Preparation of Aβ samples

Monomeric Aβ were prepared by dissolving lyophilized peptides in HFIP. The solvent of HFIP was evaporated under gentle nitrogen steam. The above Aβ was re-dissolved with DMSO and stored at −20 °C as the stock solution. Aβ monomers were freshly prepared by diluting the stock solutions with NaOH

Analyst Accepted Manuscript

This journal is © The Royal Society of Chemistry 20xx

View Article Online
DOI: 10.1039/C9AN02285F

Published on 13 January 2020. Downloaded by Queen Mary, University of London on 1/13/2020 1:30:57 PM.

(10 mM) to 2 mM, and then being diluted to the desired concentrations with PBS (10 mM, pH 7.4). The oligomeric forms of Aβ were prepared by incubating Aβ monomer solution in PBS at 37°C for 24 h.

Fabrication of functionalized gold microelectrode.

Gold microelectrodes (diameter: 12.5 μm) were bought from CH instruments Co., Ltd. (Shanghai, China). Firstly, the cleaned microelectrode was immersed in 10 mM cysteamine solution for 6 h at 4°C, which was symbolized as GME/cys. Subsequently, it was soaked in EDC/NHS activated hemin solution (0.25 mM) for 6 h to obtain a hemin-functionalized gold microelectrode (GME/cys/hemin).

Electrochemical detection of Aβ monomers

Firstly, GME/cys/hemin was incubated with 10 μL of monomeric Aβ solutions ($Aβ_{-16}$: $Aβ_{-40}$: $Aβ_{-42}$ solutions = 3:6:1) for 10 min.[33] Then, 100 μL of Cu^{2+}-PEI/AuNPs-hemin solution was added to the aforementioned monomeric Aβ solution. The electrode was incubated with the mixture for additional 40 min. After rinsing with water, silver nanoparticles was deposited by dropping 10 μL of silver enhancer solutions on the above electrode surface for 4 min in a dark incubator. Then, the electrode was rinsed with water and the linear sweep voltammogram (LSV) was recorded in 1 M KCl solution.

Electrochemical Detection of Aβ monomer level in CSF

All animal procedures were approved by the Animal Ethics Committee of East China Normal University and performed in accordance with the ARRIVE guidelines[34]. Male C57BL/6J mice and APP/PS1 double transgenic mice at 3, 8 months of age were purchased from Shanghai Research Center for Model OrganisBILITm. The mice were housed on a 12:12 h light/dark schedule with food and water ad libitum. CSF samples were taken from the cisterna magna according to the reported method.[35] Briefly, after anesthetized with sodium pentobarbital (50 mg kg^{-1}, i.p.), the mouse was positioned beneath a dissecting microscope. The meninges overlying the cisterna magna was exposed by removing the musculature from the base of the skull to the first vertebrae. The tissue above the cisterna magna is excised carefully and the residual blood or other interstitial fluid were removed. Finally, CSF samples were taken from the cisterna magna with a microneedle carefully avoiding bleeding due to damage to blood vessels. The CSF samples were diluted 100 times with PBS (10 mM, pH 7.4) for the following measurements.

Results and discussion

Synthesis of the Cu^{2+}-PEI/AuNPs-hemin nanoprobes

As a starting point of our study, Cu^{2+}-PEI/AuNPs-hemin nanoprobes were synthesized.[36,37] Initially, polyethylenimine (PEI) functionalized gold nanoparticles (PEI/AuNPs) with an average diameter of 11 nm were prepared (Figure 2A). Then, the surface of PEI/AuNPs were covalently modified with Cu^{2+} and hemin to produce dual-functionalized AuNPs (Cu^{2+}-PEI/AuNPs-hemin). As shown in Figure 2B, Cu^{2+}-PEI/AuNPs-hemin remained well dispersed while the average particle size increased to 15 nm due to the massive assembly of hemin. Zeta (ζ) potential analysis (Figure S1) revealed that the potential value of PEI/AuNPs was +37.9 mV, which agreed well with the positively charged amino groups of PEI in PBS (pH=7.4). Subsequently, the ζ potential decreased to +29.6 mV upon addition of hemin, which was negatively charged in PBS. After chelation with Cu^{2+}, the ζ potential of the obtained Cu^{2+}-PEI/AuNPs-hemin nanoprobes increased to +31.5 mV. UV−visible spectroscopy (UV−vis) has also been carried out to characterize the synthesis step (Figure 2D). Compared with PEI/AuNPs (curve a), a red shift of the absorption peak and a broader absorption band were observed on the UV−vis of Cu^{2+}-PEI/AuNPs-hemin (curve b), revealing the effect of surface molecules on metal nanoparticles.[38] All these results confirmed the successful formation of Cu^{2+}-PEI/AuNPs-hemin nanoprobes.

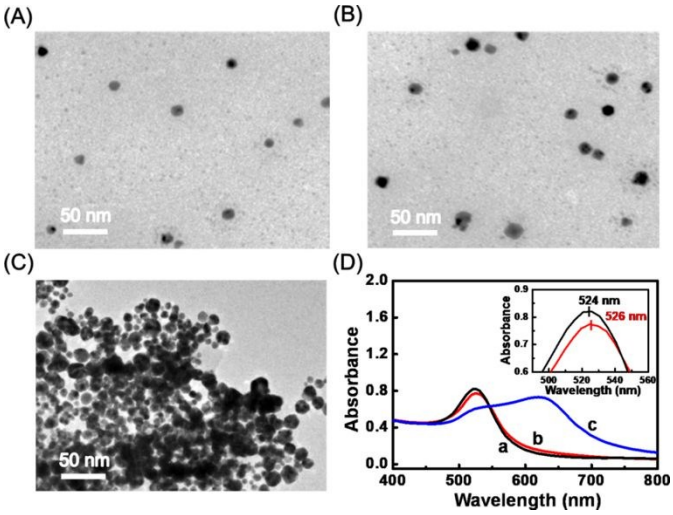

Figure 2. TEM images of (A) PEI/AuNPs, (B) Cu^{2+}-PEI/AuNPs-hemin nanoprobes and (C) Cu^{2+}-PEI/AuNPs-hemin nanoprobes in the presence of 1 μM Aβ monomers. (D) UV−vis spectra of (a) PEI/AuNPs, Cu^{2+}-PEI/AuNPs-hemin (b) before and (c) after incubated with 1 μM Aβ monomers.

Colorimetric detection of Aβ monomers

Recent studies invoked that Aβ can bind with both heme and Cu^{2+} simultaneously through high affinity. The specificity of the dual-functionalized nanoprobe (Cu^{2+}-PEI/AuNPs-hemin) was demonstrated to be applicable to Aβ monomers ($Aβ_{-16}$, $Aβ_{-40}$ and $Aβ_{-42}$).[39] Figure 3A displayed the color of Cu^{2+}-PEI/AuNPs-hemin changed from red to purple and then to blue-gray with the increased concentration of Aβ monomers. Corresponding UV−vis spectra displayed the solution of Cu^{2+}-PEI/AuNPs-hemin had a maximal absorbance at 526 nm. The successive addition of Aβ monomers decreased the absorbance peak at 526 nm and increased absorbance peak close to 610 nm. Control experiments displayed negligible changes in the spectrum upon addition of PBS (10 mM) and NaOH (10 mM) (Figure S2). Notably, TEM image exhibited remarkable aggregation of Cu^{2+}-

Analyst Accepted Manuscript

View Article Online
DOI: 10.1039/C9AN02285F

Published on 13 January 2020. Downloaded by Queen Mary, University of London on 1/13/2020 1:30:57 PM.

PEI/AuNPs-hemin nanoprobes in the presence of 1 μM Aβ monomers (Figure 2C). In addition, the average hydrodynamic sizes of Cu^{2+}-PEI/AuNPs-hemin nanoprobes changed from ~ 18 nm to ~ 265 nm (Figure S3). These results revealed the spectrum change was attributable to the Aβ-induced aggregation of Cu^{2+}-PEI/AuNPs-hemin nanoprobes. Moreover, no obvious changes were observed in the UV-vis spectra of PEI/AuNPs, PEI/AuNPs-Cu^{2+}, and PEI/AuNPs-hemin toward the same concentration of Aβ monomers (Figure S4), validating the indispensability of the dual recognition molecules in the Cu^{2+}-PEI/AuNPs-hemin nanoprobes for specific monitoring of Aβ monomers by forming Cu^{2+}-Aβ-hemin complex. The ratio of A_{610} nm/A_{526} nm was utilized for quantification of Aβ monomers and the detection range from 50 pM to 1 μM was obtained for this colorimetric sensor (Figure 3B). However, it is necessary to develop a novel technique with higher sensitivity for analysis of real sample.

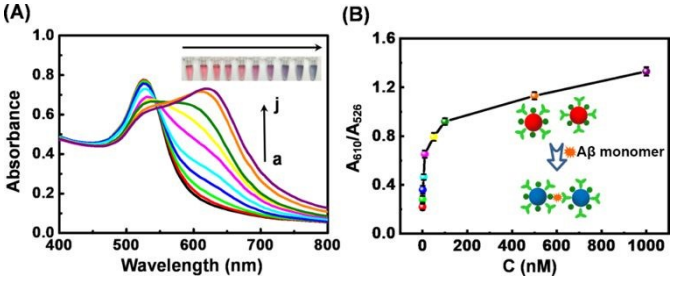

Figure 3. (A) UV–vis spectra of Cu^{2+}-PEI/AuNPs-hemin nanoprobes with different concentrations of Aβ monomers (a–i: 0, 0.05, 0.2, 1, 5, 10, 50, 100, 500 and 1000 nM). (B) Calibration curve for $A_{610\ nm}/A_{526\ nm}$ value versus Aβ monomers concentrations. Inset: photographic images of the color change of Cu^{2+}-PEI/AuNPs-hemin nanoprobes upon addition of Aβ monomers with different concentrations.

Characterization of the Functionalized Electrode

In comparison with colorimetric method, electrochemical sensing may be an alternative to further improve the sensitivity. Besides, gold microelectrodes can be engineered with an interface chemistry similar to that of AuNPs. Therefore, the process of Aβ-directed aggregation of Cu^{2+}-PEI/AuNPs-hemin nanoprobes was transferred to the gold electrode surface and converted colorimetric assay into enhanced electrochemical analysis. Initially, cysteamine was immobilized onto the surface of gold microelectrode through Au-S bond (GME/cys), followed by the modification of hemin (GME/cys/hemin) using the EDC/NHS strategy. Electrochemical impedance spectroscopy (EIS), a widely used technique for characterization of molecular assembly on electrode surfaces, was employed for investigating the fabrication procedure.[40,41] The diameter of semicircular portion in EIS was equivalent to the R_{ct} and could be calculated by fitting Randles circuit. As shown in Figure 4A, the R_{ct} of GME/cys decreased (curve b) compared with that of the bare gold microelectrode (curve a). This may result from the electrostatic interaction between the positively charged cysteamine and the negatively charged redox probe ($[Fe(CN)_6]^{3-/4-}$), which promoted the enrichment of $[Fe(CN)_6]^{3-/4-}$ on microelectrode surface and thus facilitated the electron transfer of redox probe. Then, the R_{ct} of GME/cys/hemin remarkably increased (curve c) because hemin modified on the electrode restrained the electron transfer of $[Fe(CN)_6]^{3-/4-}$. After being exposed to Cu^{2+}-PEI/AuNPs-hemin nanoprobes in the presence of Aβ monomers, the R_{ct} of GME/cys/hemin increased (curve d). X-ray photoelectron spectroscopy (XPS) exhibited characteristic peaks of Cu 2p (Figure S6A). Besides, scanning electron microscopy images (SEM) displayed a remarkable conglomeration of nanoprobes on the electrode surface (Figure 4D). These results revealed that GME/cys/hemin could capture Aβ monomers and Cu^{2+}-PEI/AuNPs-hemin nanoprobes based on hemin-Aβ-Cu^{2+} coordination between the microelectrode and nanoprobes. Then, surface-tethered Cu^{2+}-PEI/AuNPs-hemin nanoprobes can capture more Aβ as well as other nanoprobes, promoting the aggregation of AuNP on the electrode surface. The above results confirmed the successful construction of functionalized microelectrode and the feasibility for enrichment of Aβ monomers through the assembly of Cu^{2+}-PEI/AuNPs-hemin nanoprobes on microelectrode surface, which was favorable for the monitoring of Aβ monomers with low-abundance in CSF.

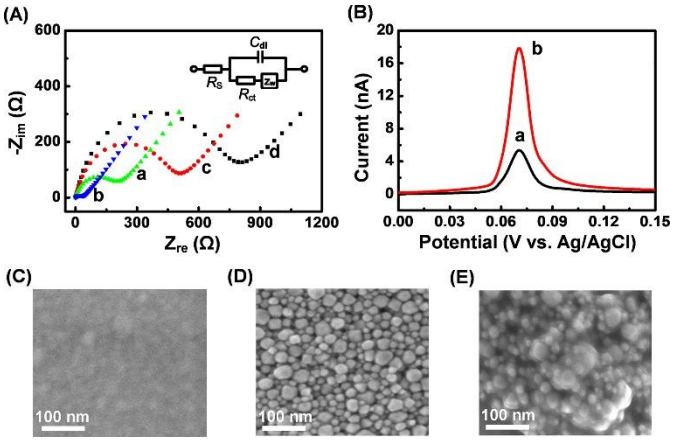

Figure 4. (A) Nyquist plots obtained at (a) GNE surface, (b) GNE/cys surface, GNE/cys/hemin surface (c) before and (d) after being incubated with Cu^{2+}PEI/AuNPs-hemin nanoprobes in the presence of 1 μM Aβ monomers. Inset: equivalent circuit used for analyzing the impedance spectra for electrochemical sensor. R_s = solution resistance, R_{ct}=charge-transfer resistance, C_{dl}=double layer capacitance, and Z_W=Warburg impedance. (B) Linear sweep voltammetry (LSV) curves of the deposited silver nanoparticles on GNE/cys/hemin incubated with Cu^{2+}-PEI/AuNPs-hemin nanoprobes (a) in the absence and (b) presence of 1 μM Aβ monomers. SEM images of (C) GNE/cys/hemin surface, (D) Cu^{2+}-PEI/AuNPs-hemin-based architecture on GNE/cys/hemin surface and (E) the silver deposition on Cu^{2+}-PEI/AuNPs-hemin-based architecture.

To sensitively detect and quantify Aβ monomers, linear-sweep voltammetry (LSV), a powerful tool for characterizing trace metal nanoparticles, was further employed based on the change of stripping peak current. Compared with AuNPs, silver

Analyst Accepted Manuscript

This journal is © The Royal Society of Chemistry 20xx

View Article Online
DOI: 10.1039/C9AN02285F

Published on 13 January 2020. Downloaded by Queen Mary, University of London on 1/13/2020 1:30:57 PM.

nanoparticles (AgNPs) can be oxidized at more negative potential with a sharp peak, which is beneficial for avoiding the interference of reducing species and improving the detection sensitivity.[42] Considering the large surface area and high catalysis activity, the Cu^{2+}-PEI/AuNPs-hemin-based architecture formed on electrode surface can in situ promote the deposition of AgNPs. Therefore, Cu^{2+}-PEI/AuNPs-hemin-catalyzed Ag deposition was utilized for further amplifying the electrochemical signal. Figure 4B showed a small signal was obtained in LSV in the absence of Aβ. After treatment with Aβ monomers, a large electrochemical signal with sharp peak was obtained. SEM image illustrated that the particle size in AuNPs architecture increased obviously (Figure 4E) and a new peak corresponding to Ag element generated in EDX (Figure S5). In addition, XPS also confirmed the production of Ag (Figure S7B). These results verified that the AuNPs-based architecture induced by Aβ recognition promoted the deposition of AgNPs on the microelectrode surface and the signal amplification of Aβ monomer detection can be achieved.

Enhanced Electrochemical Detection of Aβ monomers

Under the optimum conditions (Figure S7), the LSV responses of AgNPs deposited on the AuNPs-based architecture were utilized for quantifying Aβ monomers. Figure 5A displayed that the peak current increased as the concentration of Aβ monomers increased. A good linearity between the peak current and the logarithm of concentrations of Aβ monomers exist in the range from 1 pM to 50 nM [I_p (nA) = 13.504+ 2.533logC (nM), R^2 = 0.995] (Figure 5B). The limit of detection was 0.2 pM, which was lower than that of Cu^{2+}-PEI/AuNPs-hemin nanoprobes-based colorimetric method. The excellent sensitivity can be attributed to the dual signal amplification mechanism. The formation of AuNPs assembly not only promoted the enrichment of Aβ monomers on electrode surface but also induced the in-situ deposition of AgNPs, which can be detected with LSV for electrochemical stripping analysis of Aβ monomers. Compared with traditional electrochemical method, this technique based on microelectrode can detect Aβ solution with small volume (10 μL), which was more suitable for clinical diagnosis of real samples.

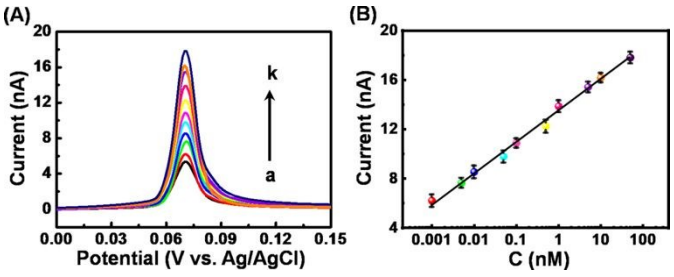

Figure 5. (A) LSV responses of GNE/cys/hemin treated with different concentrations of Aβ monomers (a–k: 0, 1 pM, 5 pM, 10 pM, 50 pM, 0.1 nM , 0.5 nM, 1 nM, 5 nM, 10 nM, 50 nM). (B) Calibration curve for the peak current value vs Aβ monomers concentrations.

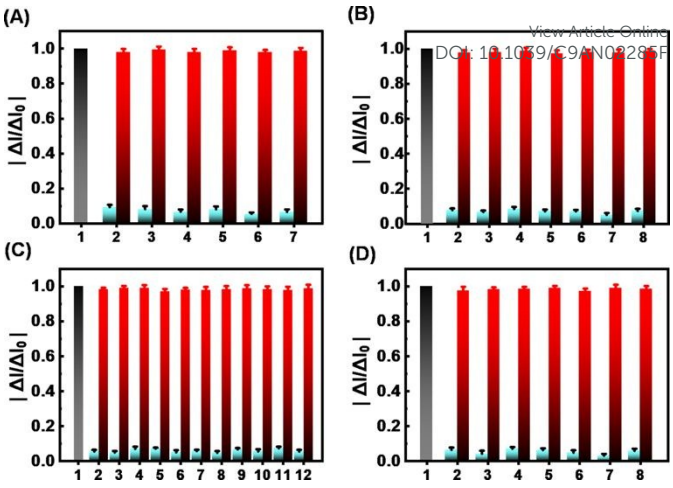

Figure 6. Selectivity and competition experiments of the electrochemical method toward (A) proteins (1–7: Aβ monomers, Tau, Actin, α-syn, Pre, VDAC1, Aβ oligomers, 1 nM for Aβ monomers and oligomers, 0.2 mg/mL for other proteins), (B) metal ions (1–8: Aβ monomers, K^+, Ca^{2+}, Na^+, Mg^{2+}, Fe^{3+}, Cu^{2+}, Zn^{2+}, 1 mM for K^+, Ca^{2+}, Na^+, Mg^{2+}; 10 μM for other metal ions; 1 nM for Aβ monomers), (C) amino acids (1–12: Aβ monomers, Glu, Gly, Phe, Ser, Val, Cys, His, Iso, Arg, Lys, Thr, 10 μM for all the tested amino acids, 1 nM for Aβ monomers). (D) other biological molecules (1–8: 1 nM Aβ monomers, 50 μM AA, 20 μM UA, 20 μM DA, 50 μM DOPAC, 20 μM 5-HT, 1 mM glucose, 1 mM lactate). The blue bars represent the ratio between the peak current change induced by potential interferences and the peak current change induced by Aβ monomers. The red bars refer to the peak current change upon addition of both potential interferences and Aβ monomers divided by the peak current change induced by Aβ monomers. ΔI_0 represents the peak current change induced by Aβ monomers, ΔI represents the peak current change induced by potential interferences or the mixture of potential interference and Aβ monomers.

The complexity of the brain system presents a great challenge for analytical performance not only in sensitivity, but also in selectivity. Therefore, the selectivity for Aβ monomers was examined by determining the peak current change ratio ($\Delta I/\Delta I_0$) arising from potential interferences against that for Aβ monomers (Figure 6). The potential interferences were checked, including some endogenic proteins, Aβ oligomers, metal ions, amino acids and other biological species that commonly coexist in biological system. These interferences showed negligible responses. For the competition test, the electrochemical response for Aβ monomers exhibited no significant changes upon the addition of the above compounds. The high selectivity may be ascribed to the strategy of analyte-recognition-mediated interfacial regulation, which can avoid the nonspecific adsorption of potential interferences onto electrode surface.[21] Furthermore, repeatability was measured by investigating the current responses of six different electrodes toward the same concentration of Aβ monomers.

Analyst Accepted Manuscript

Published on 13 January 2020. Downloaded by Queen Mary, University of London on 1/13/2020 1:30:57 PM.

The relative standard deviation was 1.0%, revealing good reproducibility of GME/cys/hemin (Figure S8).

Monitoring β-amyloid Peptides in Mouse Cerebrospinal Fluid (CSF)

It has been reported that monomeric Aβ aggregated into oligomers or fibrils during the progress of AD. Monitoring the metabolism of Aβ monomers in CSF may provide more insight into AD pathogenesis. The remarkable analytical performance of the developed method incited us to further monitor Aβ monomer level in central nervous system. The variations of Aβ monomer level in CSF among normal and AD mice were listed in Table 1. Compared with normal mice, the concentration of Aβ monomers of AD mice declined clearly. Furthermore, the Aβ monomers level was lowest for AD mice at 8 months of age. These results demonstrated the peptide accumulation was a progressive course, and consequently the amount of soluble Aβ monomers was reduced. Moreover, this method displayed a potential application for clinical analysis, which was beneficial for the exploration of AD pathogenesis.

Table 1. Evaluation of the variations in Aβ monomer levels in CSF of normal and AD mice (n = 5, mean ± S.D.)

Aβ (nM)	3 months age	8 months age
Normal	4.5±0.2	4.1±0.1
AD	3.4±0.1	1.2±0.3

Conclusions

In summary, an ultrasensitive electrochemical biosensor for monitoring Aβ monomers was proposed based on the Aβ-induced assembly of AuNPs into structured aggregates on microelectrode through the specific Cu^{2+}-Aβ-hemin coordination. The assembly of AuNPs not only facilitated the enrichment of Aβ monomers on small-sized microelectrode but also promoted the deposition of silver nanoparticles for electrochemical analysis of Aβ monomers with amplified electrochemical signal. The present method with remarkable analytical performance was proved for efficient monitoring of Aβ monomers in cerebrospinal fluid. Taking advantages of the simple principle and easy operation of diverse metal nanoparticles, the present work can also be extended to construct microelectrode interface for ultra-sensitive monitoring of other biological species related to brain disease, providing great promise for clinical studies.

Conflicts of interest

There are no conflicts to declare.

Acknowledgements

This work was supported by National Natural Science Foundation of China (No. 21974048, 21675053, 21635003), Science and Technology Commission of Shanghai Municipality (No. 19ZR1414600 and 18DZ1112700), and China Scholarship Council (No. 201806145043).

View Article Online DOI: 10.1039/C9AN02285F

Notes and references

1 Gravina, S.; Ho, L.; Eckman, C.; Long, K.; Jr, L.; Younkin, L.; Suzuki, N.; Younkin, S. Amyloid β Protein (Aβ) in Alzheimeri's Disease Brain Biochemical and immunocytochemical analysis with antibodies specific for forms ending at $Aβ_{40}$ or $Aβ_{42\ (43)}$. *J. Biol. Chem.* 1995, **270**, 7013-7016.

2 Hamley, I.W; The amyloid beta peptide: a chemist's perspective. Role in Alzheimer's and fibrillization. *Chem. Rev.,* 2012, **112**, 5147-5192.

3 Zhou, Y.; Liu, L.; Hao, Y.; Xu, M. Detection of Aβ monomers and oligomers: early diagnosis of Alzheimer's disease. *Chem. Asian. J.*, 2016, **11**, 805-817.

4 Hardy, J.; Selkoe, D. The amyloid hypothesis of Alzheimer's disease: progress and problems on the road to therapeutics. *Science,* 2002, **297**, 353-356.

5 Hamley, I. Peptide fibrillization. *Angew. Chem. Int. Ed.,* 2007, **46**, 8128-8147.

6 Wiltfang, J.; Smirnov, A.; Schnierstein, B.; Kelemen, G.; Matthies, U.; Klafki, H.; Staufenbiel, M.; Hüther, G.; Rüther, E.; Kornhuber, J. Improved electrophoretic separation and immunoblotting of beta-amyloid (Aβ) peptides 1-40, 1-42, and 1-43. *Electrophoresis*, 1997, **18**, 521-532.

7 Näslund, J.; Haroutunian, V.; Mohs, R.; Davis, K.; Davies, P.; Greengard, P.; Buxbaum, J. Correlation between elevated levels of amyloid β-peptide in the brain and cognitive decline. *JAMA*, 2000, **283**, 1571-1577.

8 Lanz, T.; Schachter, J. Demonstration of a common artifact in immunosorbent assays of brain extracts: Development of a solid-phase extraction protocol to enable measurement of amyloid-β from wild-type rodent brain. *J. Neurosci. Meth.,* 2006, **157**, 71-81.

9 Xia, N.; Liu, L.; Harrington, M.; Wang, J.; Zhou, F. Regenerable and simultaneous surface plasmon resonance detection of $Aβ_{(1–40)}$ and $Aβ_{(1–42)}$ peptides in cerebrospinal fluids with signal amplification by streptavidin conjugated to an n-terminus-specific antibody. *Anal. Chem.,* 2010, **82**, 10151-10157.

10 Hanger, D.; Betts, J.; Loviny, T.; Blackstock, W.; Anderton, B. New phosphorylation sites identified in hyperphosphorylated tau (paired helical filament-tau) from Alzheimer's disease brain using nanoelectrospray mass spectrometry. *J. Neurochem.,* 1998, **71**, 2465-2476.

11 Watanabe, K.; Ishikawa, C.; Kuwahara, H.; Sato, K.; Komuro, S.; Nakagawa, T.; Nomura, N.; Watanabe, S.; Yabuki, M. A new methodology for simultaneous quantification of total-Aβ, $Aβ_{x-38}$, $Aβ_{x-40}$, and $Aβ_{x-42}$ by column-switching LC/MS/MS. *Anal. Bioanal. Chem.,* 2012, **402**, 2033-2042.

12 Picou, R.; Moses, J.; Wellman, A.; Kheterpal I.; Gilman, S. Analysis of monomeric $Aβ_{(1–40)}$ peptide by capillary electrophoresis. *Analyst,* 2010, **135**, 1631-1635.

13 Zhou, Y.; Dong, H.; Liu, L.; Xu, M. Simple Colorimetric Detection of Amyloid β-peptide (1–40) based on Aggregation of Gold Nanoparticles in the Presence of Copper Ions. *Small,* 2015, **11**, 2144-2149.

14 Hu, T.; Chen, C.; Huang, G.; Yang, X. Antibody modified-silver nanoparticles for colorimetric immuno sensing of $Aβ_{(1–40/1–42)}$ based on the interaction between β-amyloid and Cu^{2+}. *Sensor. Actuat. B,* 2016, **234**, 63-69.

15 Luo, Y.; Zhang, L.; Liu, W.; Yu, Y.; Tian, Y. A Single Biosensor for Evaluating the Levels of Copper Ion and L-Cysteine in a Live Rat Brain with Alzheimer's Disease. *Angew. Chem. Int. Ed.,* 2015, **54**, 14053-14056.

16 Gu, H.; Hou, Q.; Liu, Y.; Cai, Y.; Guo, Y.; Xiang, H.; Chen, S. On-line regeneration of electrochemical biosensor for in vivo

Analyst Accepted Manuscript

This journal is © The Royal Society of Chemistry 20xx

View Article Online
DOI: 10.1039/C9AN02251F

repetitive measurements of striatum Cu^{2+} under global cerebral ischemia/reperfusion events. *Biosens. Bioelectron.,* 2019, **135**, 111-119.

17 Yu, Y.; Zhang, L.; Li, C.; Sun, X.; Tang, D.; Shi, G. A Method for Evaluating the Level of Soluble β-Amyloid$_{(1–40/1–42)}$ in Alzheimer's Disease Based on the Binding of Gelsolin to b-Amyloid Peptides. *Angew. Chem. Int. Ed.,* 2014, **53**, 1-5.

18 Wu, F.; Yu, P.; Mao, L. Bioelectrochemistry for in vivo analysis: Interface engineering toward implantable electrochemical biosensors. *Current Opinion in Electrochemistry*, 2017, **5**, 152-157.

19 Hutton, E.; Ogorevc, B.; Hočevar, S.; Smyth, M. Bismuth film microelectrode for direct voltammetric measurement of trace cobalt and nickel in some simulated and real body fluid samples. *Anal. Chim. Acta.,* 2006, **557**, 57-63.

20 Lei, J.; Ju, H. Signal amplification using functional nanomaterials for biosensing. *Chem. Soc. Rev.,* 2012, **41**, 2122-2134.

21 Li, M.; Lv, M.; Wang, L.; Fan, C.; Zuo, X. Engineering electrochemical interface for biomolecular sensing. *Current Opinion in Electrochemistry,* 2019, **14**, 71-80.

22 Sage, A.; Besant, J.; Lam, B.; Sargent, E.; Kelley, S. Ultrasensitive electrochemical biomolecular detection using nanostructured microelectrodes, *Accounts. Chem. Res.,* 2014, **47**, 2417-2425.

23 Pramanik, D.; Ghosh, C.; Dey, S. Heme–Cu bound Aβ peptides: spectroscopic characterization, reactivity, and relevance to Alzheimer's Disease. *J. Am. Chem. Soc.,* 2011, **133**, 15545-15552.

24 Dong, H.; Zou, F.; Hu, X.; Zhu, H.; Koh, K.; Chen, H. Analyte induced AuNPs aggregation enhanced surface plasmon resonance for sensitive detection of paraquat. *Biosens. Bioelectron.,* 2018, **117**, 605-612.

25 Wei, T.; Dong, T.; Wang, Z.; Bao, J.; Tu, W.; Dai, Z. Aggregation of Individual Sensing Units for Signal Accumulation: Conversion of Liquid-Phase Colorimetric Assay into Enhanced Surface-Tethered Electrochemical Analysis. *J. Am. Chem. Soc.,* 2015, **137**, 8880-8883.

26 Park, S.; Taton, T.; Mirkin, C. Array-based electrical detection of DNA with nanoparticle probes. *Science*, 2002, **295**, 1503-1506.

27 Wang, J.; Xu, D.; Polsky, R. Magnetically-induced solid-state electrochemical detection of DNA hybridization. *J. Am. Chem. Soc*., 2002, **124**, 4208-4209.

28 He, Y.; Xie, S.; Yang, X.; Yuan, R.; Chai, Y. Electrochemical Peptide Biosensor Based on in Situ Silver Deposition for Detection of Prostate Specific Antigen. *ACS Appl. Mater. Inter.,* 2015, **7**, 13360-13366.

29 Toh, H.; Batchelor-McAuley, C.; Tschulik, K.; Uhlemann, M.; Crossley, A.; Compton, R. The anodic stripping voltammetry of nanoparticles: electrochemical evidence for the surface agglomeration of silver nanoparticles. *Nanoscale,* 2013, **5**, 4884-4893.

30 Chu, X.; Fu, X.; Chen, K.; Shen, G.; Yu, R. An electrochemical stripping metalloimmunoassay based on silver-enhanced gold nanoparticle label. *Biosens. Bioelectron.,* 2005, **20**, 1805-1812.

31 Chumbimuni-Torres, K.; Dai, Z., Rubinova, N.; Xiang, Y.; Pretsch, E.; Wang, J.; Bakker, E. Potentiometric biosensing of proteins with ultrasensitive ion-selective microelectrodes and nanoparticle labels. *J. Am. Chem. Soc.,* 2006, **128**, 13676-13677.

32 Veerakumar, P.; Velayudham, M.; Lu, K.; Rajagopal, S. Polyelectrolyte encapsulated gold nanoparticles as efficient active catalyst for reduction of nitro compounds by kinetic method. *Appl. Catal. A: Gen.,* 2012, **439**, 197-205.

33 Liu, L.; He, Q.; Zhao, F.; Xia, N.; Liu, H.; Li, S.; Liu, R.; Zhang, H. Competitive electrochemical immunoassay for detection of β-amyloid (1–42) and total β-amyloid peptides using p-aminophenol redox cycling. *Biosens. Bioelectron.,* 2014, **51**, 208-212.

34 Kilkenny, C.; Browne, W.; Cuthill, I.; Emerson, M.; Altman, D. Improving bioscience research reporting: the ARRIVE guidelines for reporting animal research. *PLoS Biol.*, 2010, **8**, e1000412.

35 Meyding-Lamadé, U.; Ehrhart, K.; de Ruiz, H.; Kehm, R.; Lamadé, W. A new technique: serial puncture of the cisterna magna for obtaining cerebrospinal fluid in the mouse--application in a model of herpes simplex virus encephalitis. *J. Exp. Anim. Sci.,* 1996, **38**, 77-81.

36 Hu, W.; Yu, X.; Hu, Q.; Kong, J.; Li, L.; Zhang, X. Methyl orange removal by a novel PEI-AuNPs-hemin nanocomposite. *J. Environ. Sci*., 2017, **53**, 278-283

37 Zhao, W.; Jia, W.; Sun, M.; Liu, X.; Zhang, Q.; Zong, C.; Qu, J.; Gai, H. Colorimetric detection of Cu^{2+} by surface coordination complexes of polyethyleneimine-capped Au nanoparticles. *Sensor. Actuat. B-Chem.,* 2016, **223**, 411-416

38 Lim, D.; Jeon, K.; Hwang, J.; Kim, H.; Kwon, S.; Suh, Y.; Nam, J. Highly uniform and reproducible surface-enhanced Raman scattering from DNA-tailorable nanoparticles with 1-nm interior gap. *Nat. Nanotechnol.,* 2011, **6**, 452-460.

39 Yu, Y.; Zhang, L.; Sun, X; Li, C.; Qiu, Y.; Sun, H.; Tang, D.; Liu, Y.; Yin, X.; A sensitive colorimetric strategy for monitoring cerebral β-amyloid peptides in AD based on dual-functionalized gold nanoplasmonic particles. *Chem. Commun.,* 2015, **51**, 8880-8883.

40 Ding, S.; Cao, S; Zhu, A.; Shi, G. Wettability switching of electrode for signal amplification: conversion of conformational change of stimuli-responsive polymer into enhanced electrochemical chiral analysis. *Anal. Chem.,* 2016, **88**, 12219-12226.

41 Zhu, A.; Liu, Y.; Rui, Q.; Tian, Y. Selective and sensitive determination of hydroxyl radicals generated from living cells through an electrochemical impedance method. *Chem. Commun.,* 2011, **47**, 4279-4281.

42 Lin, D.; Wu, J.; Wang, M.; Yan, F.; Ju, H. Triple signal amplification of graphene film, polybead carried gold nanoparticles as tracing tag and silver deposition for ultrasensitive electrochemical immunosensing. *Anal. Chem.,* 2012, **84**, 3662-3668.

Published on 13 January 2020. Downloaded by Queen Mary, University of London on 1/13/2020 1:30:57 PM.

Analyst Accepted Manuscript

View Article Online
DOI: 10.1039/C9AN02285F

TOC

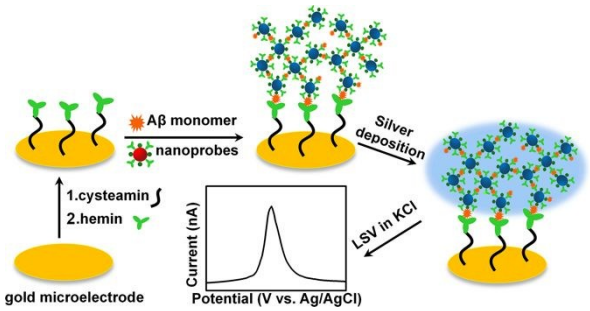

Aβ monomer directed the assembly of Cu^{2+}-PEI/AuNPs-hemin nanoprobes into network aggregates on microelectrode interface for enhanced electrochemical analysis.

Published on 13 January 2020. Downloaded by Queen Mary, University of London on 1/13/2020 1:30:57 PM.

Analyst Accepted Manuscript